Analysis of *osm-6*, a Gene That Affects Sensory Cilium Structure and Sensory Neuron Function in *Caenorhabditis elegans*

Joan Collet,*† Caroline A. Spike,* Erik A. Lundquist,*,[1] Jocelyn E. Shaw* and Robert K. Herman*

**Department of Genetics and Cell Biology, University of Minnesota, St. Paul, Minnesota 55108 and †Centre d'Investigació i Desenvolupament, Consell Superior d'Investigaciones Científiques, Barcelona, Spain*

Manuscript received July 23, 1997
Accepted for publication September 15, 1997

ABSTRACT

Mutation in the *Caenorhabditis elegans* gene *osm-6* was previously shown to result in defects in the ultrastructure of sensory cilia and defects in chemosensory and mechanosensory behaviors. We have cloned *osm-6* by transposon tagging and transformation rescue and have identified molecular lesions associated with five *osm-6* mutations. The *osm-6* gene encodes a protein that is 40% identical in amino acid sequence to a predicted mammalian protein of unknown function. We fused *osm-6* with the gene for green fluorescent protein (GFP); the fusion gene rescued the *osm-6* mutant phenotype and showed accumulation of GFP in ciliated sensory neurons exclusively. The OSM-6::GFP protein was localized to cytoplasm, including processes and dendritic endings where sensory cilia are situated. Mutations in other genes known to cause ciliary defects led to changes in the appearance of OSM-6::GFP in dendritic endings or, in the case of *daf-19*, reduced OSM-6::GFP accumulation. We conclude from an analysis of genetic mosaics that *osm-6* acts cell autonomously in affecting cilium structure.

CILIA are found in most animal species, many protozoa and some plants. Many cilia are motile. Motile cilia can sweep fluid over an epithelial surface or propel a swimming cell; the eukaryotic flagellum, which is related to the cilium in structure, is also used for swimming, as in the green alga Chlamydomonas or in the sperm of many species. Nonmotile cilia are found in certain sensory receptors, including phototransducing rods and cones and olfactory neurons.

The nematode *Caenorhabditis elegans* has no motile cilia or flagella—its sperm, for example, are nonflagellated crawling cells (Wolf *et al.* 1978; Nelson and Ward 1980). Nonmotile cilia, however, are present in 60 of the 302 neurons that make up the nervous system of the *C. elegans* hermaphrodite (Ward *et al.* 1975; Ware *et al.* 1975; Perkins *et al.* 1986; White *et al.* 1986; Hall and Russell 1991). The cilia are situated in dendritic endings of sensory neurons. Most of the ciliated nerve endings are either exposed directly to the external environment or embedded in the animal's external cuticle and are strongly implicated, by two lines of evidence, in the reception of chemosensory and mechanosensory stimuli.

One line of evidence implicating *C. elegans* cilia in sensory transduction involves mutants with structurally abnormal cilia (Lewis and Hodgkin 1977; Albert *et al.* 1981; Perkins *et al.* 1986). Such mutants are defective in the ability to sense chemical attractants or repellants, both water soluble and volatile (reviewed in Bargmann and Mori 1977). They are also defective in the ability to avoid high osmolarity (Culotti and Russell 1978). The ability to form dauer larvae under conditions of limited food and high concentration of a pheromone secreted by a dense population of worms (reviewed in Thomas 1993; Riddle and Albert 1997) is another chemosensory behavior that is defective in mutants with aberrant cilia. Also affected is the ability to recover from the dauer state, which involves the sensing of food and low pheromone concentration. Finally, cilia-defective mutants are mechanosensory defective: they show a reduced ability to respond to taps on their noses (Kaplan and Horvitz 1993). Although it is possible that the cilia-defective mutants are also defective in a nonciliary neuron function, the simplest view is that cilia are directly involved in transducing chemosensory and mechanosensory signals.

The second line of evidence is based on the behavioral consequences of killing cilia-containing neurons with a laser microbeam. These experiments have focused attention on particular ciliated neurons as sensory receptors; the roles of the ciliated endings are inferred. Thus, different subsets of ciliated neurons have been implicated in the ability to chemotax to water-soluble attractants (Bargmann and Horvitz 1991a) or volatile odorants (Bargmann *et al.* 1993), to avoid repellents (Bargmann *et al.* 1990), to form dauer larvae or not and to recover from the dauer state (Bargmann

Corresponding author: Robert K. Herman, Department of Genetics and Cell Biology, University of Minnesota, 250 BioScience Center, 1445 Gortner Avenue, St. Paul, MN 55108.
[1]*Present address:* Department of Anatomy, University of California, San Francisco, CA 94143-0452.

and Horvitz 1991b; Schackwitz *et al.* 1996). Killing a subset of ciliated neurons also reduces the ability to respond to nose taps (Kaplan and Horvitz 1993).

Cilia-defective mutants provide a powerful approach to the interesting question of how cilia are assembled. This approach has been fruitful in elucidating the assembly of Chlamydomonas flagella, for example (reviewed in Johnson 1995). Mutations in the *C. elegans* gene *osm-6* result in shortened axonemes of all cilia that have been inspected by serial section electron microscopy (Perkins *et al.* 1986). The base of each cilium, which corresponds to the transition zone of the Chlamydomonas flagellum, is ultrastructurally normal in the *osm-6* mutant, but the region distal to the transition zone is greatly reduced in length, and doublet microtubules, linked to the cell membrane, assemble ectopically at positions proximal to the transition zone. It has been proposed that the ectopic microtubules are misassembled components of the axoneme and that the *osm-6* gene product may be required for the assembly of peripheral microtubule doublets on the ciliary template (Perkins *et al.* 1986). We report here our cloning and molecular characterization of *osm-6* and its spatial pattern of expression. We also describe our mosaic analysis of *osm-6* function.

MATERIALS AND METHODS

General genetic methods, genes and alleles: Growth media and culture and mating techniques were as described by Brenner (1974) and Sulston and Hodgkin (1988). Nematode strains were grown and mated at 20° unless otherwise noted. Nomenclature is standard (Horvitz *et al.* 1979). Genes and mutations used in this work were the following (where no citation is given, see Hodgkin *et al.* 1988): LG (linkage group) I: *che-3(e1124)*, *che-13(e1805)*. LGII: *daf-19(m86)*. LGIII: *ncl-1(e1865)*, *unc-36(e251)*, *sup-5(e1464)*, *dpy-18(e364)*. LGIV: *osm-3(p802)*, *daf-10(e1387)*, *him-8(e1489)*. LGV: *unc-42(e270)*, *daf-11(m47*, *m87*ts*)*, *osm-6(p811*, *m511*, *m533*, *m201*, *sa119)* (Starich *et al.* 1995), *smal-1(e30)*, *che-11(e1810)*, *vab-8(e1017)*. LGX: *che-2(e1033)*, *osm-5(p813)*, *osm-1(p808)*. Except for the strain in which the spontaneous mutations *osm-6(m511)* and *osm-6(m533)* arose, which was RW7097, a derivative of RW7096 (Mori *et al.* 1988), all strains descended from the wild-type strain N2 (Brenner 1974).

Mutations in *osm-6* abolish the ability of 12 anterior and four posterior sensory neurons in living animals to fill with the fluorescent dyes 5-fluorescein isothiocyanate (FITC) or 3,3′-dioctadecyloxacarbocyanine perchlorate (DiO) (Hedgecock *et al.* 1985; Perkins *et al.* 1986; Starich *et al.* 1995). We used this defect in dye filling, the Dyf phenotype, to follow *osm-6* mutations in genetic crosses. To reduce Tc1 copy number, the original strains carrying *osm-6(m511)* and *osm-6(m533)* were crossed to N2 males. Heterozygous hermaphrodite progeny were allowed to give self-progeny, among which Dyf (homozygous *osm-6*) animals were identified to initiate new lines. This procedure was carried out at least 10 times for each mutation, after which a *him-8; unc-42 osm-6* strain was generated for each mutation. In addition, *unc-42 osm-6 vab-8* stocks were generated for each of the two Tc1-insert mutations, and crossovers on each side of *osm-6* were selected to reduce the number of closely linked Tc1 elements.

Assays for neuronal filling of FITC or DiO and behavioral assays for chemotaxis and ability to form dauer larvae were performed as described by Starich *et al.* (1995).

Identification and outcrossing of spontaneous *osm-6* revertants: Each of the mutator strains bearing one of the spontaneous mutations *osm-6(m511)* or *osm-6(m533)* was screened for spontaneous reversion of the defect in dauer larva formation, the Daf-d phenotype, conferred by the *osm-6* mutation. Dauer larvae formed in starved cultures were selected, as described by Starich *et al.* (1995), by virtue of their resistance to 1% sodium dodecyl sulfate (SDS) (Cassada and Russell 1975). Selected dauer larvae were allowed to recover in the presence of food, and the resulting stocks were scored for dye filling. Several independent revertants from each mutant, all both non-Daf-d and non-Dyf, were identified. The following procedure, described for a specific example, was used to reduce the Tc1 copy number of several revertants. Hermaphrodites of genotype *him-8; unc-42 osm-6(m533)*, which had been outcrossed to N2 or N2-derived strains at least 12 times, as described in the preceding section, were mated with *him-8* males, and the male cross-progeny were mated to *osm-6(m533mn374)* (revertant) hermaphrodites. F_1 hermaphrodites were picked and allowed to self. From broods containing Unc-42 Dyf animals, generated by *him-8; unc-42 osm-6(m533)/osm-6(m533mn374)* hermaphrodites, non-Unc animals were picked. Those that segregated no Unc self-progeny were picked, from which a *him-8; osm-6(m533mn374)* line was established. Males of this line were mated with *him-8; unc-42 osm-6(m533)* hermaphrodites. Non-Unc male progeny were backcrossed to *him-8; unc-42 osm-6(m533)* hermaphrodites. The last step was repeated at least 10 times. At each step, it was determined that Unc segregants were Dyf and non-Unc segregants were non-Dyf. After the final cross, homozygous *him-8; unc-42 osm-6(m533)* and *him-8; unc-42 osm-6(m533mn374)* stocks were established.

Molecular biology: Standard molecular biology techniques (Sambrook *et al.* 1989) were used. Two *C. elegans* cDNA libraries were used: a λgt10 mixed-stage library provided by S. Kim and a λZAP mixed-stage library provided by R. Barstead and R. Waterston. All plasmid subcloning was done using pBlueScript SK(−) (Stratagene, La Jolla, CA). DNA was sequenced by the dideoxy chain termination method (Sanger *et al.* 1977) using Sequenase Version 2.0 (United States Biochemical, Cleveland, OH). Deletion series of clones for sequencing were obtained by timed exonuclease III digestion (Henikoff 1987). Sequence analysis made use of the Genetics Computer Group (Madison, WI) sequence analysis package and the National Center for Biotechnology Information BLAST (Altschul *et al.* 1990) service. For Northern blot analysis, poly(A)-enriched RNA was isolated from staged populations of N2 animals as described by Starich *et al.* (1993).

Cloning Tc1-tagged *osm-6*: Genomic DNA was prepared as previously described (Li *et al.* 1992) from N2 and outcrossed strains carrying either of the spontaneous mutations *m511* or *m533* or a reversion of one of these mutations. Southern blots were probed with radioactively labeled Tc1 probe, as described by Starich *et al.* (1993), and a 2.8-kb Tc1-containing *Eco*RI restriction fragment derived from an *osm-6(m533)* strain was subcloned. Tc1 sequence in the clone was removed by *Eco*RV digestion (Rosenzweig *et al.* 1983) to create a plasmid carrying unique sequence flanking *m533::Tc1*, which was used to screen an N2 λEMBL4 genomic library provided by C. Link.

Germline transformation and *osm-6* rescue: Hermaphrodites homozygous for *osm-6(p811)* were transformed by the method of Mello *et al.* (1991). DNA to be tested was injected at 10–15 μg/ml, and plasmid pRF4, which contains the semidominant mutation *rol-6(su1006)*, was coinjected at 80 μg/ml. Transgenic roller (Rol) hermaphrodites were picked, from which

stably transformed lines were recovered and scored for dye filling. Lines that showed rescue of *osm-6* exhibited essentially wild-type dye filling and amphid and phasmid neurons. The following four different genomic DNA fragments were tested for rescue of *osm-6* (Figure 1C): pJC4 is a 5.9-kb *Bam*HI restriction fragment; pJC5 was made by deleting 1.2 kb from one end of pJC4 by exonuclease III digestion (Henikoff 1987); pJC17 is a 3.7-kb *Eco*RI/*Bam*HI subfragment from pJC4; and pJC35 was made to carry a frameshift mutation within the proposed *osm-6* coding region (which generates downstream stop codons) by digesting pJC4 with *Bcl*I, end-filling with Klenow enzyme and religating. We confirmed the DNA sequence of pJC35 in the vicinity of the frameshift mutation.

DNA sequence determination of *osm-6* mutations: Purified DNA from *osm-6* mutants was amplified by polymerase chain reaction (PCR) using Taq polymerase (Promega, Madison, WI). We amplified the genomic region extending from 85 bp upstream of the 5′ end of the *osm-6* cDNA to 37 bp downstream of the deduced *osm-6* translational stop. Cloned PCR products were sequenced using gene-specific oligonucleotide primers. Mutations were confirmed by sequencing products from at least two different PCRs.

Testing amber suppressibility of *osm-6(sa119)*: The *osm-6(sa119)* mutation was originally identified (Starich *et al.* 1995) as a suppressor of the dauer constitutive phenotype Daf-c, conferred by *daf-11(m87*ts*)* at high temperature. Because *osm-6* and *daf-11* are only 0.2 map unit apart, the following steps were taken to recover *osm-6(sa119)* by itself. Unc non-Sma recombinants segregating from *unc-42 sma-1/daf-11 osm-6* hermaphrodites were picked, and self-progeny homozygous for *osm-6* were identified by dye-filling assay. The presence or absence of *daf-11(m87)* was ascertained by mating animals to be tested with *him-8; daf-11(m47)* males at 25° and inspecting the cross-progeny for dauer larvae; four of 24 Unc non-Sma Osm recombinants were *daf-11(+)*. A strain carrying only *osm-6(sa119)* was then obtained following mating of *unc-42 osm-6* hermaphrodites with N2 males.

To test the ability of *sup-5* to suppress *osm-6(sa119)*, we crossed males of genotype *sup-5 dpy-18/++* to *dpy-18; unc-42 osm-6(sa119)* hermaphrodites. Dpyish (one copy of *sup-5* partially suppresses the homozygous *dpy-18* mutation; see Waterston 1981) non-Unc progeny were picked, from which Unc non-Dpy (fully suppressed) self-progeny, genotype *sup-5 dpy-18; unc-42 osm-6*, were identified; these animals exhibited partial dye filling, much better than *osm-6(sa119)* but not completely wild type. Completely Dyf (*osm-6*) Unc animals, genotype *unc-42 osm-6*, were recovered from this stock following mating with N2 males.

Expression experiments: A translational fusion of *osm-6* and a green fluorescent protein (GFP) gene (Chalfie *et al.* 1994), *gfp*, was constructed in the *gfp* expression vector pPD95.77 (A. Fire, S. Xu, J. Ahnn and G. Seydoux, personal communication). Included upstream of *gfp* in the fusion gene was 5.1 kb of *osm-6* genomic sequence, extending from 2.4 kb upstream of the 5′ end of the *osm-6* cDNA through the first 10 exons and all introns into the last exon, such that only the last 13 codons, including the translational stop, of OSM-6 were lacking. The *osm-6* sequence was composed of three conjoined segments (from left to right in Figure 1C): a 2.68-kb *Bam*HI genomic restriction fragment that extends upstream of the 5′ end of the *osm-6* cDNA into the second *osm-6* intron, a 2.17-kb *Bam*HI/*Bgl* II genomic fragment that extends from the same *Bam*HI site in the second intron to a *Bgl* II site in the last exon, and a 0.22-kb cDNA fragment that extends from the same *Bgl* II site to a 3′ truncation produced by exonuclease III digestion that deleted the 12 C-terminal amino acid codons of OSM-6.

Extrachromosomal arrays carrying the *osm-6::gfp* construct and either *rol-6(su1006)* (see section on germline transformation above) or *unc-36(+)* (see section on mosaic analysis below) as visible markers were generated by germline transformation via microinjection of DNA. Lines homozygous for an integrated array bearing *osm-6::gfp* and *unc-36(+)* were identified among F_2 descendants of *unc-36 ncl-1 III; osm-6(p811) V; mnEx64[osm-6::gfp unc-36(+)]* hermaphrodites treated with γ-rays, by the procedure described by Mello and Fire (1995).

Mosaic analysis: Animals of genotype *ncl-1 unc-36 III; osm-6(p811) V* were made transgenic for an extrachromosomal array, *mnEx54*, containing wild-type copies of *osm-6* on pJC4, *ncl-1* on the cosmid C33C3 (Miller *et al.* 1996) and *unc-36* on the plasmid R1p16 (obtained from L. Lobel). The *mnEx54* array rescued the Dyf phenotype conferred by *osm-6(p811)*. Non-Unc animals were exposed to DiO and examined by Nomarski differential interference contrast (DIC) microscopy to screen for mosaics in which some neurons of an amphid were Ncl (enlarged nucleolus) and others were non-Ncl. When mosaics were found, various cells were scored with respect to both dye filling and the Ncl phenotype. Nuclei were identified using published diagrams. (Albertson and Thomson 1976; Sulston and Horvitz 1977; Sulston *et al.* 1983; White *et al.* 1986). Cell names and lineages are given by Sulston and White (1988).

RESULTS

All five *osm-6* mutant alleles confer a strong Dyf phenotype: The *osm-6* gene is represented by five mutant alleles (Culotti and Russell 1978; Starich *et al.* 1995), all recessive to *osm-6(+)*. The reference allele, *p811*, has been shown to cause defects in osmotic avoidance (Culotti and Russell 1978), chemotaxis (Perkins *et al.* 1986; Starich *et al.* 1995), dauer larva formation (Perkins *et al.* 1986) and mechanosensation (Kaplan and Horvitz 1993), and it was the allele that was used in the characterization of axonemal shortening caused by *osm-6* mutation (Perkins *et al.* 1986). We have monitored another phenotype conferred by *osm-6* mutation. When living wild-type animals are exposed to a fluorescent dye, either FITC or DiO, eight pairs of sensory neurons—six in head sensilla called amphids and two in phasmids in the tail—fill with the dye (Hedgecock *et al.* 1985); *osm-6* mutation abolishes dye filling (Perkins *et al.* 1986), a phenotype referred to as Dyf. For each of the five *osm-6* mutations, we have assayed hundreds of homozygous hermaphrodites for their ability to take up DiO. For either adults or larvae bearing any of the *osm-6* mutations, more than 99% of the animals failed to exhibit dye filling of any amphid or phasmid neuron. By contrast, among more than 2000 wild-type hermaphrodites, the great majority exhibited characteristic dye filling, and no animal failed completely to dye fill. It was previously reported that *osm-6(p811)* over a deficiency for the *osm-6* locus is fully Dyf (Starich *et al.* 1995). By dye-filling assay, therefore, all five *osm-6* mutations are indistinguishable and appear to behave as null mutations; it is possible that they are not null, however, and that an *osm-6* null mutant would exhibit additional defects.

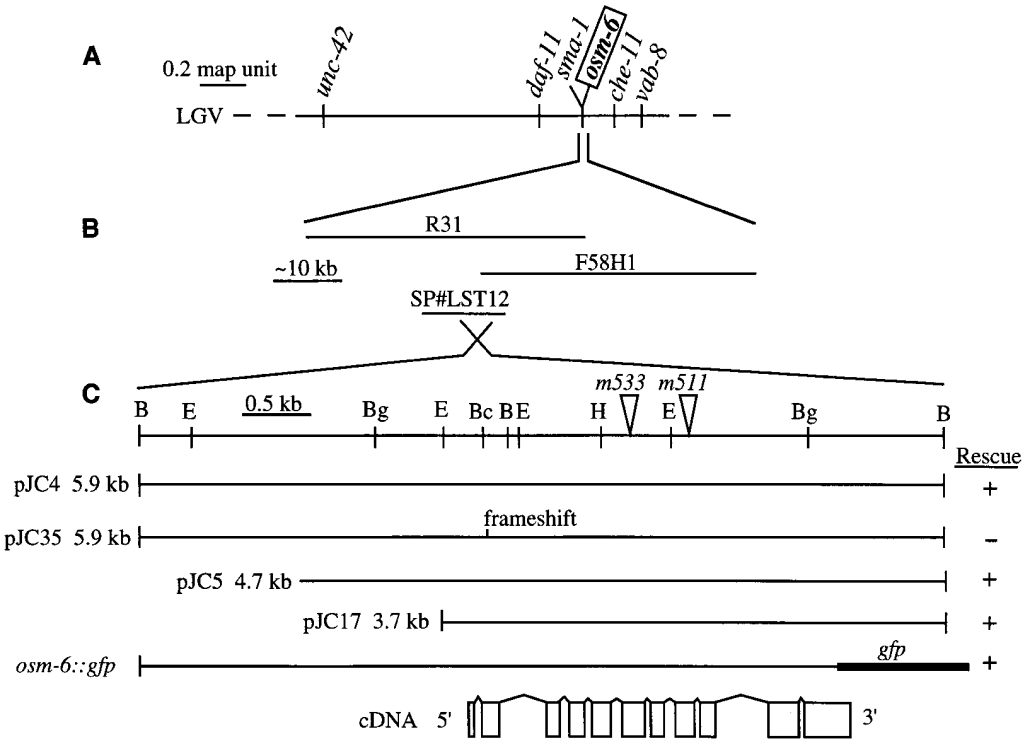

Figure 1.—Genetic and physical maps of the *osm-6* region. (A) Genetic map of a portion of linkage group V, showing relative positions of *osm-6* and closely linked genes used in this work. (B) Physical map showing relative positions of overlapping cosmids R31 and F58H1 (Coulson *et al.* 1995) and λ genomic clone SP#LST12. (C) Restriction map of a 5.9-kb fragment subcloned from SP#LST12. The map is inverted with respect to the maps in A and B. The points of insertion of the transposable element Tc1 are shown for the two mutations *m511* and *m533*. Restriction site abbreviations: B, *Bam*HI; Bc, *Bcl*I; Bg, *Bgl*II; E, *Eco*RI; H, *Hin*dIII. The cDNA exons (boxes) are appropriately positioned relative to the genomic restriction map. The *osm-6::gfp* construct is missing the 3′ untranslated region and last 12 C-terminal amino acids encoded by the *osm-6* cDNA.

Transposon tagging of *osm-6*: Two *osm-6* alleles, *m511* and *m533*, were identified (Starich *et al.* 1995) among spontaneous mutations arising in RW7097, a strain that exhibits enhanced germline transposition of the transposable element Tc1 (Mori *et al.* 1988). Several spontaneous phenotypic revertants of both *m511* and *m533* were identified, with the expectation that they could be generated by excision of Tc1. To reduce overall Tc1 copy numbers, strains harboring *m511* or *m533* were repeatedly outcrossed to N2 or N2-derived strains, and revertants of *m511* or *m533* were repeatedly outcrossed to multiply outcrossed *m511* and *m533* stocks, respectively (see materials and methods). Southern blots of DNA isolated from *m511*, *m533*, revertant and N2 stocks probed with Tc1 sequence were inspected for mutant-specific bands. Candidate Tc1-containing bands were cloned, and unique DNA fragments flanking the Tc1 elements were subcloned and used to probe Southern blots. It was found that strains bearing either *m511* or *m533* had a Tc1 element in the same 4.8-kb *Bam*HI fragment (Figure 1). The corresponding *Bam*HI fragment in N2 and all revertants had no Tc1 element and was 3.2 kb in size—reduced by 1.6 kb, the size of Tc1.

Transformation rescue of *osm-6*: Unique DNA flanking *m533::Tc1* in a 2.8-kb *Eco*RI fragment was used to screen a genomic library, and hybridizing phage clones were identified. Two of these were placed on the *C. elegans* physical map by A. Coulson and J. Sulston (Coulson *et al.* 1995), in a region that corresponds well to the expected location of *osm-6*, on the basis of its genetic map location (Figure 1).

Fragments of one of the physically mapped phage clones, SP#LST12, were subcloned and used to generate transgenic lines by germline transformation of *osm-6(p811)* (Figure 1). Transgenic lines were tested for rescue of the Dyf phenotype conferred by *osm-6(811)*. A 3.7-kb *Eco*RI/*Bam*HI fragment, which included the sites of insertion of both *m511::Tc1* and *m533::Tc1*, was capable of transformation rescue (Figure 1). We determined the DNA sequence of the rescuing fragment. The DNA sequence of the entire region was recently determined by the *C. elegans* DNA Sequence Consortium (Wilson *et al.* 1994); large portions of the two cosmids shown in Figure 1B, R31 (GenBank accession number Z75956) and F58H1 (accession number Z75954), were used in the genomic sequencing.

A 1.5-kb *osm-6* cDNA: The 3.7-kb *Eco*RI/*Bam*HI rescuing fragment was used to screen a mixed-stage, amplified cDNA library, and four identical hybridizing clones were isolated. One of these was used to screen a second mixed-stage cDNA library. One hybridizing clone was isolated; it contained less *osm-6* sequence than that found in the other cDNA clones. We determined the nucleotide sequence of both strands of one

```
                                    ↓
ATGCCTCCATTTTCAGACGAAAAGATGACTAACCGGAGTATTGGGAGAAAAGTTCTGATT   60
M  P  P  F  S  D  E  K  M  T  N  R  S  I  G  R  K  V  L  I    20

GATCAATCAAAACAGCAACAAATTAGTTTGATTAGTGGTTTTCGTGGTGTGGCAAGACAT  120
D  Q  S  K  Q  Q  Q  I  S  L  I  S  G  F  R  G  V  A  R  H    40
                           ↓
TTAAAAAGTGTTCTTACTGTTGAAATAAACACAGAACCAATTAACTTAAATGGATTAGAA  180
L  K  S  V  L  T  V  E  I  N  T  E  P  I  N  L  N  G  L  E    60
                                          ↓
GATGTTCGGATGCTTATCATTCCACAACCAAAGACATCATTTGGAACTGGAGAGATTGAA  240
D  V  R  M  L  I  I  P  Q  P  K  T  S  F  G  T  G  E  I  E    80

GCAATATGGAAGTTTGTGGAAGAAGGTGGTTCATTGATGATCCTTTCTGGTGAAGGTGGT  300
A  I  W  K  F  V  E  E  G  G  S  L  M  I  L  S  G  E  G  G    100
                                          ↓
GAGAGACAATCATTAAATGAAATGATTGCAAAATATGGAATTACTGTGAATAAGGATTCG  360
E  R  Q  S  L  N  E  M  I  A  K  Y  G  I  T  V  N  K  D  S    120

GTAATTCGTACTGTATTCCTGAAATATTTTGATCCGAAAGAAGCTTTAGTAGCAAATGGA  420
V  I  R  T  V  F  L  K  Y  F  D  P  K  E  A  L  V  A  N  G    140

GTCATAAATCGAGCAATTGCAGTGGCTGCAAAAAAGAATGTGAGCACTGAGCAAAAACAT  480
V  I  N  R  A  I  A  V  A  A  K  K  N  V  S  T  E  Q  K  H    160
      ↓
AATTCACAAGCACTTTCATTCATTTATCCATATGGATGTACTCTAGATGTGAATAATCGT  540
N  S  Q  A  L  S  F  I  Y  P  Y  G  C  T  L  D  V  N  N  R    180

ATGTCGAATGTAGTATTGTCTTCTGGAAGTACAAGTTTTCCAACAAGTCGCCCAGTTGCC  600
M  S  N  V  V  L  S  S  G  S  T  S  F  P  T  S  R  P  V  A    200
                              ↓
GCTTTTCATGAGACAAAACTCAATGAAATGAAAAAGAAAGGTAGAGTGTGTGTGGTTGGA  660
A  F  H  E  T  K  L  N  E  M  K  K  K  G  R  V  C  V  V  G    220
                                          ↓
TCAGTCTCGATGTTTCATGACACATACATCGACAAGGAAGAAAATGGAAAGATTTTTGAT  720
S  V  S  M  F  H  D  T  Y  I  D  K  E  E  N  G  K  I  F  D    240

ACATTTGTGGAATTCCTGGTCAATGGTCTTGAACTGAACACGATAGATGCTGCAGAGCCG  780
T  F  V  E  F  L  V  N  G  L  E  L  N  T  I  D  A  A  E  P    260
                                          ↓
GAAATTAATGATTACACAAATATTCCAGATCATATTCATATGTCCCAGCAGATCAAGGTT  840
E  I  N  D  Y  T  N  I  P  D  H  I  H  M  S  Q  Q  I  K  V    280

TGTATGTACGAAGGAGAATTGGATCAGGCAATCAGTTCGGATTTCATGAAGATTATGGAT  900
C  M  Y  E  G  E  L  D  Q  A  I  S  S  D  F  M  K  I  M  D    300
                                       ↓
ACTTCGTTGCATTCTTTTAATTTGAAACATTGGCCAATGACTATAAGATTGTATGAAGCA  960
T  S  L  H  S  F  N  L  K  H  W  P  M  T  I  R  L  Y  E  A    320

TTGAATCTTTCACCTCCACCACTTACCCTTGTTGAACCTCAATTTGAACTTCCAATGCCT 1020
L  N  L  S  P  P  P  L  T  L  V  E  P  Q  F  E  L  P  M  P    340

CCATTTCAACCTGCAGTATTTCCACCAACATTTCAAGAATTACCAATGCCTCCTCTTGAA 1080
P  F  Q  P  A  V  F  P  P  T  F  Q  E  L  P  M  P  P  L  E    360

TTATTTGATCTTGATGAACAGTTCAGCTCTCCGGAAATTCAACTTTCTCAGCTCGCAAAT 1140
L  F  D  L  D  E  Q  F  S  S  P  E  I  Q  L  S  Q  L  A  N    380
   ↓
AGAAGCGAGGAAGAAGATCTCATATTCTTTATTGAAAAAGCTGGTGAAATTACTGGAATA 1200
R  S  E  E  E  D  L  I  F  F  I  E  K  A  G  E  I  T  G  I    400

TCTGCTGAATTGACAAGAAGTGAACGAACCCCCAAGAAGATAATTGAGTTGGCAGTGAGC 1260
S  A  E  L  T  R  S  E  R  T  P  K  K  I  I  E  L  A  V  S    420

AAACTCATGTTATTCAAACGTTCAATGATGGATGGAGAGTTGGAAGTTGCATCAGCGTTC 1320
K  L  M  L  F  K  R  S  M  M  D  G  E  L  E  V  A  S  A  F    440

GATATTGGAGAGCATGATGCTCATCATCAAAGTTTTAATCAAGGCGAAGAGATGGACGAG 1380
D  I  G  E  H  D  A  H  H  Q  S  F  N  Q  G  E  E  M  D  E    460

CAGCTGTTCTCTGATATTGATGAGTTCGATGATTTGTGATTGATTTGTCTGGAGATAAGA 1440
Q  L  F  S  D  I  D  E  F  D  D  L  *                         472

TAATAAAATATTCATGTTGAAAAAAAAAAAAAAAAA                          1476
```

Figure 2.—Nucleotide sequence of *osm-6* cDNA and amino acid sequence encoded by the *osm-6* cDNA open reading frame (EMBL accession number AJ000259). The arrows above the cDNA sequence mark the positions of the 10 *osm-6* introns. A 34-nucleotide segment rich in proline residues is given in boldface. The two copies of a 6-nucleotide repeat in the proline-rich domain are underlined. The putative poly(A) signal is underlined near the 3′ end of the cDNA sequence. The first nine A residues in the poly(A) tail of the cDNA sequence match the *osm-6* genomic sequence.

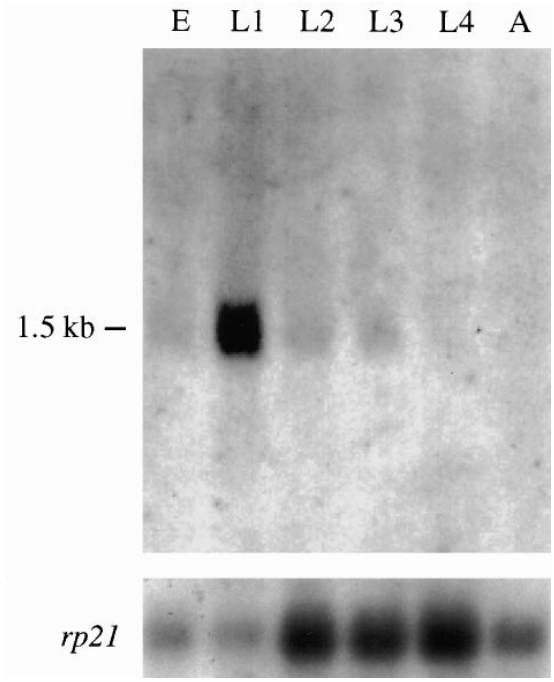

Figure 3.—An *osm-6* transcript of about 1.5 kb is most abundant at the L1 stage. RNA was isolated from eggs (E), the four larval stages (L1–L4) and young adults (A). Poly(A)-enriched RNA was hybridized to the *osm-6* cDNA as probe. To monitor the relative RNA contents of the different lanes, we hybridized the same blot to a radioactively labeled cDNA clone of the ribosomal protein gene *rp21*, provided by A. Fire.

of the four identical clones (Figure 2). Comparison of the cDNA and genomic nucleotide sequences indicated that the cDNA is composed of 11 exons, five of which (exons 4–8), as well as the coding region of exon 11, were predicted by the Sequencing Consortium (as part of predicted gene *R31.3* under GenBank accession number Z75956). All 10 introns have consensus *C. elegans* donor and acceptor splice sites (Blumenthal and Steward 1997).

We have not clearly identified the 5′ end of the *osm-6* message. The 1476-bp length of the cDNA corresponds to the approximately 1.5-kb length of the *osm-6* transcript detected on Northern blots probed with the cDNA (Figure 3). The 5′ end of the cDNA begins with an initiation codon AUG and an open reading frame that extends for 1416 nucleotides. Four codons upstream of the 5′ end of the cDNA in the genomic sequence is a stop codon, with no intervening AUG codons but with a possible intervening 3′ splice acceptor site. The rescuing DNA fragment pJC17 (Figure 1C) extends 190 nucleotides upstream of the start of the cDNA. There is only one AUG codon within this 190 nucleotides; the third in-frame codon following it is a stop, however, and no pattern of splicing with consensus splice sites puts the AUG in-frame with the rest of the *osm-6* message. We suggest that the *osm-6* translational start is included in the cDNA. The second AUG codon of the cDNA open reading frame is the ninth codon. Introduction of frameshift mutation between this AUG and the third AUG in the open reading frame (Figure 1C, codon number 64) abolished transformation rescue. We suggest that translation is initiated at a position corresponding to one of the first two AUG codons of the cDNA. The second AUG codon gives a

better match to previously identified *C. elegans* translational initiation sites (Krause 1995), but there is no strong consensus sequence for *C. elegans* translational initiation. The 3′ end of the cDNA contains a poly(A) stretch, 18 bp upstream of which is a consensus polyadenylation signal, AATAAA.

The *osm-6* transcript is most abundant during the first larval stage (Figure 3).

DNA alterations in *osm-6* mutants: We found sequence alterations associated with each of the five known *osm-6* mutant alleles (Figure 4). Each of the two Tc1 insertion mutations was within the *osm-6* coding sequence, both at TA target sites, which have been found for all Tc1 insertions (Van Luenen and Plasterk 1994). The other three mutations, all induced with ethyl methanesulfonate (EMS), were G/C-to-A/T transitions, the most common class of mutation caused by EMS in *C. elegans* (Anderson 1995). Two of the transition mutations affected splice sites: *p811* altered the splice site acceptor of the first intron, and *m201* altered the splice site donor of the seventh intron. Finally, *sa119* was associated with the change of codon 377 from glutamine encoding to a UAG or amber stop codon. Consistent with this result is our finding that the dye-filling defect conferred by *sa119* is suppressed by the amber suppressor *sup-5* (see materials and methods). As expected, neither of two other *osm-6* mutations tested, *osm-6(m511)* and *osm-6(m533)*, was amber suppressible. The genetic characterization of *sa119* as an amber-suppressible mutation confirms our molecular identification of *osm-6*.

OSM-6 is 40% identical to a predicted mammalian protein: Conceptual translation of the *osm-6* cDNA predicts a polypeptide (OSM-6) of 472 amino acids. A hydropathy profile (Kyte and Doolittle 1982) indicates that the protein has neither a signal peptide nor a transmembrane domain. Overall the protein is acidic, with a calculated isoelectric point of 4.64. The region extending from amino acid 325 through 358 is strikingly rich in proline: 13 of 34 residues. Within this segment is an exact six-residue repeat: ELPMPP appears at both 336–341 and 353–358 (Figure 2).

A search of protein databases revealed that OSM-6 is 40% identical to the conceptual translation product of a cDNA clone, called NGD5, isolated from a neuroblastoma–glioma rat–mouse hybrid cell line called NG108-15 (Wick *et al.* 1995). Comparison of the translation products of the *osm-6* cDNA and the published NGD5 sequence suggested that there were sequencing errors in the published NGD5 sequence. We therefore obtained the *NGD5* cDNA clone and determined its nucleotide sequence; conceptual translation of the corrected sequence (updated GenBank accession number L38481) gives a better match to OSM-6 (Figure 5). Transcripts corresponding to *NGD5* are reported to be decreased after prolonged treatment of NG108-15 cells with opioid (Wick *et al.* 1995). The transcript is also reported to be expressed in rat brain. The similarity between OSM-6 and the NGD5 protein extends throughout the entire length of the NGD5 protein, which is somewhat shorter than OSM-6 (Figure 5). The two N-termini would be more closely matched if translation of the *osm-6* mRNA began at the position corresponding to the second AUG of the *osm-6* cDNA. The similarity between OSM-6 and the NGD5 protein throughout the full extent of the latter is also apparent in a dot plot comparison of the two proteins (data not shown). Four regions of particularly high similarity, all with at least 75% amino acid identity, are marked in Figure 5. The longest of these, with 34 of 44 identical residues in the segment that includes OSM-6 residues 327–370, includes nearly all of the proline-rich segment.

OSM-6 was also found to be very similar to the (incomplete) conceptual translation products of 16 mammalian expressed sequence tags (ESTs). All 16 of the ESTs are highly similar, generally more than 85% iden-

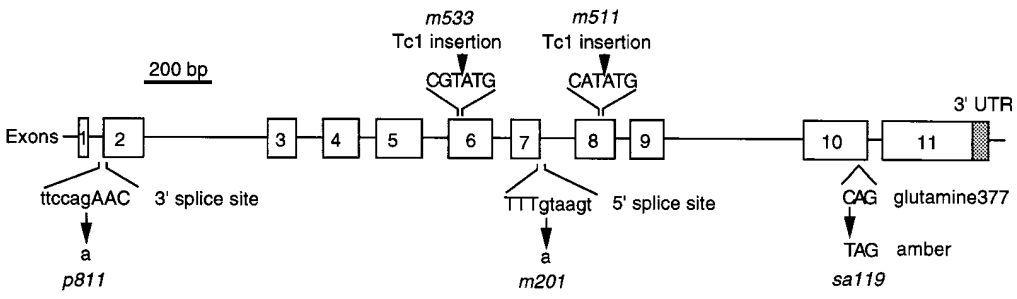

Figure 4.—DNA changes in *osm-6* mutants. Open boxes indicate exons; the stippled box represents the 3′ untranslated region of the *osm-6* mRNA. Two of the mutations were insertions of the transposable element Tc1, between nucleotides 540 and 541 of the cDNA sequence (Figure 2) for *m533* and nucleotides 819 and 820 for *m511*. All three EMS-induced mutations were G/C-to-A/T transitions, *p811* and *m201* affecting splice sites and *sa119* generating an amber nonsense mutation at codon 377 (Figure 2).

tical at the nucleotide level to different segments of the *NGD5* coding sequence. One of the ESTs was from a cDNA generated from rat PC12 cells (Lee *et al.* 1995). Two others were derived from mouse brain and mouse embryos. The remaining 13 were from cDNAs derived from several different human tissues.

***osm-6::gfp* is expressed in ciliated neurons:** To elucidate the pattern of expression of *osm-6*, we fused a GFP gene (Chalfie *et al.* 1994), *gfp*, in-frame to the 3′ end of an *osm-6* genomic segment that included 2.5 kb upstream of the beginning of the cDNA sequence and extended through the *osm-6* coding region into the last exon such that the *osm-6* translation product lacked only the 12 C-terminal amino acids. This *osm-6::gfp* translational fusion gene was injected into the germline of *osm-6* hermaphrodites, and extrachromosomal arrays were generated. Some arrays carried a dominant *rol-6* allele as a marker and others carried *unc-36(+)* (see materials and methods). Two *rol-6*-bearing lines and one *unc-36(+)*-bearing line were studied with respect to patterns of GFP expression. From the *unc-36(+)*-bearing line, several independent lines were created in which the *osm-6::gfp* array was integrated and homozygous in an otherwise *unc-36; osm-6(p811)* genome. Three of these lines were studied with respect to patterns of GFP expression. The patterns of GFP expression were analyzed in more detail for the three integrated lines, but the patterns were essentially identical for all the lines we studied. We tested one of the *rol-6*-bearing lines and an integrated *unc-36(+)*-bearing line for rescue of the DiO dye-filling defect; both exhibited excellent rescue. The same integrated *unc-36(+)*-bearing line was also tested for its abilities to chemotax up a radial gradient of NH_4Cl and to make dauer larvae; it was well rescued, exhibiting wild-type behavior, with respect to both of these characteristics (data not shown).

```
OSM-6 MPPFSDEKMTNRSIGRKVLIDQSKQQQISLISGFRGVARHLKSVLTVEIN  50
NGD5  .........MEKELRSTILFNAYKKEVFTTNTGYKSLQKRLRSNWKIQSL  41

OSM-6 TEPINLNGLEDVRMLIIPQPKTSFGTGEIEAIWKFVEEGGSLMILSGEGG 100
NGD5  KDEITSEKLIGVKLWITAGPREKFTAAEFEVLKKYLDSGGDILVMLGEGG  91

OSM-6 ERQ...SLNEMIAKYGITVNKDSVIRTVFLKYFDPKEALVANGVINRAIA 147
NGD5  ESRFDTNINFLLEEYGIMVNNDAVVRNVYYKYFHPKEALVSDGVLNREIS 141

OSM-6 VAAKKNVST.....EQKHNSQALSFIYPYGCTLDVNNRMSNVVLSSGSTS 192
NGD5  RAAGKAVPGVIDEENSGNNAQALTFVYPFGATLSVMKP.AVAVLSTGSVC 190

OSM-6 FPTSRPVAAFHETKLNEMKKKGRVCVVGSVSMFHDTYIDKEENGKIFDTF 242
NGD5  FPLNRPILAFYHSKNQGF...GKLAVLGSCHMFSDQYLDKEENSKIMDVV 237

OSM-6 VEFLVNG.LELNTIDAAEPEINDYTNIPDHIHMSQQIKVCMYEGELDQAI 291
NGD5  FQWLTTGDIHLNQIDAEDPEISDYTMVPDTATLSEQLRVCLQEGDEN... 284

OSM-6 SSDFMKIMDTSLHSFNLKHWPMTIRLYEALNLSPEPLTLVEPQFELPMPP 341
NGD5  PRDFTTLFDLSIYQLDTTCLPKVIKAHEELNVKHEPLQLVQPQFEMPLPA 334

OSM-6 FQPAVFPPTFQELPMPPLELFDLDEQFSSPEIQLSQLANRSEEEDLIFFI 391
NGD5  LQPAVFPPSFRELPPPPLELFDLDETFSSEKARLAQITNKCTDEDLEFYV 384

OSM-6 EKAGEITGISAELTRSERTPKKIIELAVSKLMLFKRSMMDGELEVASAFD 441
NGD5  RKCGDILGVTSKLPKDQQDAKHILEHIFFQVVEFKKLNQEAH         426

OSM-6 IGEHDAHHQSFNQGEEMDEQLFSDIDEFDDL                    472
```

Figure 5.—Comparison, based on the Gap program of the Genetics Computer Group, of conceptual translation products of *osm-6* and a mammalian cDNA clone, *NGD5*. Gaps in either sequence introduced to optimize alignment are indicated by intervening dots in sequence. Identical residues are joined by lines; related residues are joined by single or double dots. In the alignment shown, 40% of the amino acid residues in the NGD5 sequence are identical to OSM-6 residues. Four ungapped segments in which more than 75% of the residues are identical are indicated by boxes.

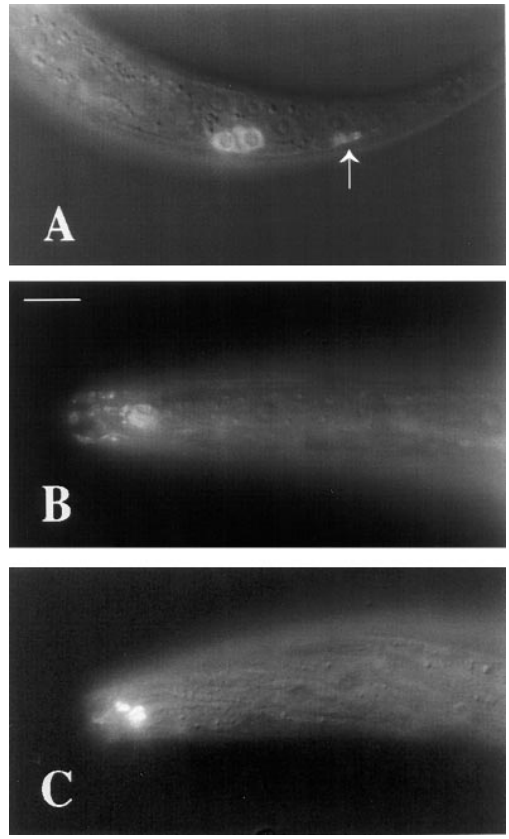

Figure 6.—Localization of OSM-6::GFP in wild-type and mutant animals, as detected by fluorescence microscopy. The images are composites of fluorescence and DIC micrographs. (A) GFP fluorescence is apparent in the cell bodies of two wild-type right phasmid neurons, PHAR and PHBR, and also in the region of the dendritic endings of the neurons (indicated by the arrow), posterior to the cell bodies. The cell nuclei tend to exclude OSM-6::GFP; this is an L2 animal. (B) GFP fluorescence in the anterior of an L4 wild-type hermaphrodite. The large patch of fluorescence correspond to the positions of cilia of other sensory neurons. The cell bodies of these neurons are at more posterior positions (to the right and out of the field of the micrograph). (C) GFP fluorescence in an L4 *che-3* mutant. Enhanced fluorescence is concentrated in a patch associated with amphid neurons and is much brighter than the corresponding region in wild-type animals (exposure times for the different fluorescent images were not equivalent). Magnifications in all panels are the same; scale bar is 10 μm.

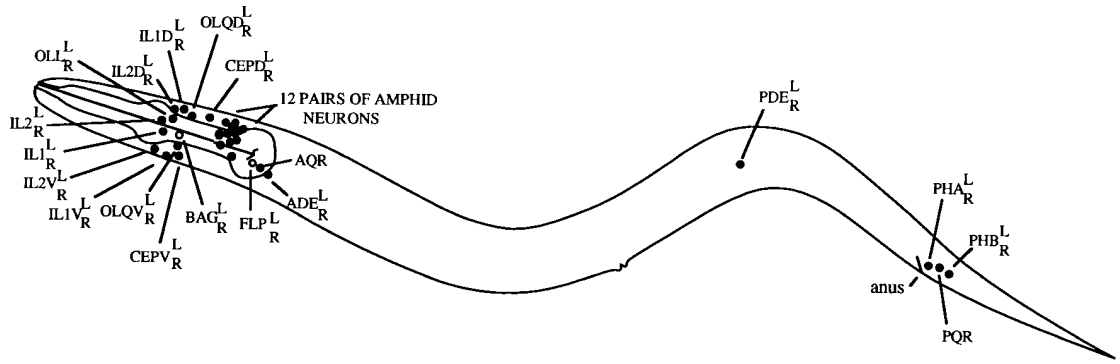

Figure 7.—Positions of nuclei of all ciliated neurons in the *C. elegans* hermaphrodite (White *et al.* 1986). All but two of the 60 neurons are members of bilateral pairs and are represented in the diagram by a single cell; for example, immediately posterior to the anus is the pair of cells PHAL (on the left side) and PHAR (on the right). The two asymmetric ciliated neurons are AQR, which is on the right side near the posterior bulb of the pharynx, and PQR, which is on the left side in the tail. We have detected GFP expression by an *osm-6::gfp* construct in 56 cells of the hermaphrodite, all of the ciliated neurons except the BAG and FLP pairs (indicated in the drawing by open circles).

GFP in the *osm-6::gfp*-bearing animals was first apparent at about the twofold stage of embryonic elongation. L1 animals showed strong expression, which then gradually weakened during larval development. This pattern is consistent with the appearance of *osm-6* transcript assessed by Northern blot analysis (Figure 3). By switching between Nomarski and fluorescence microscopy while maintaining a particular field of view, we were able to identify all GFP-expressing cells in hermaphrodites. The assignments were based primarily on the relative positions of nuclei, as shown in published diagrams (Sulston *et al.* 1983; White *et al.* 1986), but we were also aided by the appearance of GFP in neuronal processes, the characteristic shapes of which have been documented for every neuron in the hermaphrodite (Ward *et al.* 1975; Ware *et al.* 1975; White *et al.* 1986; Hall and Russell 1991).

We have detected GFP expression in a total of 56 cells in hermaphrodites, all neurons (Figures 6 and 7). These were the 24 amphid neurons, 12 inner and six outer labial neurons, the bilateral neuron pairs CEPV, CEPD, ADE, PDE, PHA and PHB and the two asymmetric neurons AQR and PQR. Four of the GFP-expressing neurons did not exhibit expression until after hatching. AQR and PQR first showed expression during the mid- to late L1 stage, which is consistent with their postembryonic origin as descendants of QR and QL, respectively (Sulston and Horvitz 1977; Sulston and White 1988). Similarly, the pair of PDE neurons are generated during the L2 stage, which is when we first saw their GFP expression.

A common feature of the GFP-expressing neurons is that they make sensory cilia (White *et al.* 1986); a diagram showing the positions of the nuclei of the 60 ciliated neurons of the hermaphrodite is given in Figure 7. We did not detect GFP expression in four additional cilium-containing neurons, the BAG and FLP pairs.

The appearance of GFP within cells that expressed the *osm-6::gfp* fusion gene was clearly cytoplasmic, as could be seen in the cell bodies of the GFP-expressing neurons (Figure 6A). In addition to the appearance of GFP within cell bodies, there was GFP along processes and near the ciliated endings (Figure 6). This is particularly apparent in the nose, which is abundantly endowed with ciliated endings.

We have analyzed, in less detail, *osm-6::gfp* expression in males. It appears that all of the cells that expressed GFP in hermaphrodites also did so in males, but male-specific GFP-expressing cells were also apparent. Four of these were ciliated neurons in the head, the CEM or male-specific cephalic neurons, which differentiate from cells that are eliminated in the hermaphrodite by embryonic cell death (Sulston *et al.* 1983). Additional cells in the male tail expressed GFP. At least some of these cells appear to be sensory neurons of the copulatory spicules and sensory rays (Sulston *et al.* 1980), since we observed GFP fluorescence associated with the endings of the spicules and rays (Figure 8). The sensory ray and spicule dendrites terminate in short cilia (Sulston *et al.* 1980; Chow *et al.* 1995; D. Hall, personal communication).

The localization of OSM-6::GFP near sensory cilia is affected by mutations in other genes that affect cilia structure: The appearance of GFP in wild-type and *osm-6* mutant backgrounds was indistinguishable; however, the *osm-6::gfp* array rescues the *osm-6* mutant phenotype. For other mutant backgrounds, we chose reference mutations in other genes that affect the structure of ciliated neurons. For *che-2*, *che-13*, *osm-1* and *osm-5* mutants, whose sensory cilia, like those of *osm-6*, are all severely foreshortened (Lewis and Hodgkin 1977; Perkins *et al.* 1986), the intensity of GFP fluorescence in the tips of the neurons was greatly reduced, although GFP accumulation in the neuron cell bodies

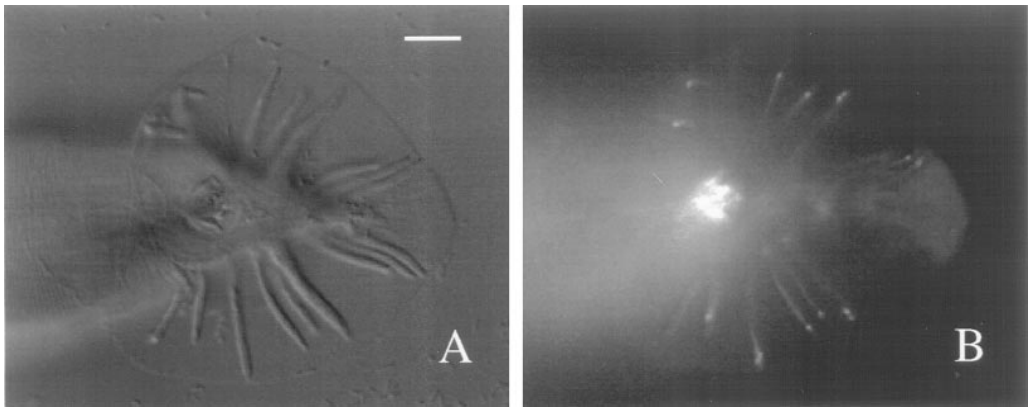

Figure 8.—GFP accumulation in tips of sensory rays of male tail promoted by *osm-6::gfp*. (A) Nomarski micrograph. (B) Fluorescence, showing fluorescent ray tips (and a patch of autofluorescence in the region of the cloaca). Scale bar is 10 μm.

appeared to be the same as in the wild-type genetic background. We did not discern an altered pattern of OSM-6::GFP expression in *osm-3* animals, but only amphid and phasmid cilia are foreshortened in the *osm-3* mutant and not to the same degree as in *che-2*, *che-13*, *osm-1* and *osm-5* mutants (Perkins *et al.* 1986). The *osm-3* gene, which encodes a kinesin-like protein, appears to be expressed in a limited subset of ciliated neurons, including eight pairs of amphid neurons (Tabish *et al.* 1995). Animals mutant for *che-3*, which encodes a dynein heavy chain (W. Grant, personal communication), showed enhanced GFP accumulation in two large bilateral patches near the region of the dendritic endings of the amphid neurons (Figure 6C) and also near the phasmid endings. Ultrastructural analysis of *che-3* mutants has shown that the amphid (and phasmid) cilia are reduced in length and have bulb-shaped endings filled with electron-dense material (Lewis and Hodgkin 1977; Albert *et al.* 1981); we thus suggest that OSM-6::GFP is associated with the bulb-shaped endings. OSM-6::GFP expression in *daf-10* and *che-11* mutants also showed patches of GFP expression in the neuronal endings that were thicker than wild-type, although they were not as large as the patches seen in *che-3* mutants. This pattern is also consistent with electron microscopic studies, which have shown that at least some cilia are enlarged in diameter and contain ground material in their centers (Albert *et al.* 1981; Perkins *et al.* 1986).

All sensory dendrites in *daf-19* mutants are devoid of cilia, including transition zones (Perkins *et al.* 1986). The number of sensory neurons exhibiting GFP accu-

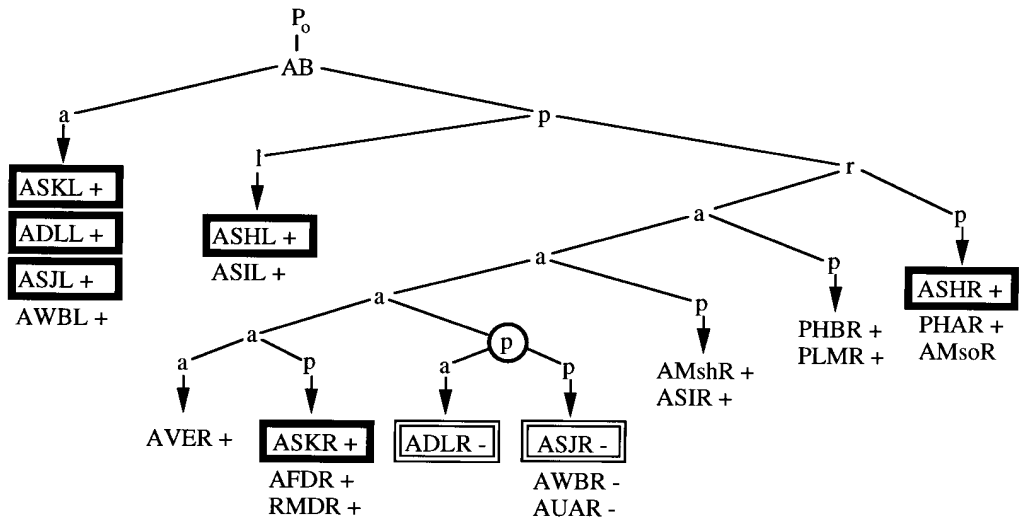

Figure 9.—Example of an *osm-6* genetic mosaic. The partial cell lineages of 21 cells are shown. Cell and lineage nomenclature follows Sulston and White (1988). The zygote P_0 contained an extrachromosomal array carrying *ncl-1(+)*, *unc-36(+)* and *osm-6(+)* and was otherwise *ncl-1 unc-36; osm-6*. The Ncl phenotypes of various scored cells are given as minus or plus, for Ncl and non-Ncl, respectively. It is concluded that the cell ABpraaap, indicated in the lineage diagram by a circled p, failed to transmit the array to its descendants, which were as a consequence all Ncl. Four bilateral pairs of amphid neurons were scored with respect to their DiO-filling phenotype. Two neurons in the right amphid, ADLR and ASJR, both of which are descended from ABpraaap, failed to fill with dye, as indicated by the double-lined boxes. The other six neurons, ASKR and ASHR in the right amphid and all four left amphid neurons, did fill with DiO, as indicated by the heavily lined boxes. Note that both the right amphid sheath, AMshR, and socket, AMsoR (although not scored explicitly with respect to its Ncl phenotype), must have carried *osm-6(+)* but did not prevent the loss of dye filling by the two *osm-6* right amphid neurons. This and other examples led to the conclusion that *osm-6* affects dye filling cell autonomously. The two right phasmid neurons, PHAR and PHBR, were both non-Ncl and, as expected, filled with DiO (for simplicity, their dye-filling phenotypes are not indicated in the diagram).

mulation in *daf-19* animals was less than half that found in wild-type. We scored only a few cells, but amphid neurons ASK, ADL and ASI and phasmid neurons PHA and PHB rarely, if ever, accumulated detectable GFP in *daf-19* animals.

***osm-6* acts cell autonomously with respect to dye filling of amphid neurons:** Our expression studies, which indicate that OSM-6 is a cytoplasmic protein present in precisely those neurons that exhibit ultrastructural defects in *osm-6* mutants, predict that *osm-6* functions cell autonomously. We tested this prediction by generating *osm-6* genetic mosaics and asking about the *osm-6* focus of action with respect to dye filling of amphid neurons.

To generate *osm-6* mosaics, we made *unc-36 ncl-1 III; osm-6 V* animals transgenic for an extrachomosomal DNA array, *mnEx54*, that contained wild-type copies of *unc-36*, *ncl-1* and *osm-6*. The extrachromosomal array was subject to mitotic loss. Each loss generated a clone of mutant cells, and the *ncl-1* mutation, which results in enlarged nucleoli, a phenotype referred to as Ncl, was used as a cell-autonomous marker for specifying the nature of mosaic animals (Hedgecock and Herman 1995; Miller *et al.* 1996). The focus of action of *unc-36* is among the descendants of both daughters of ABp (Kenyon 1986), the posterior daughter of AB, which is one of the two descendants of the first embryonic cleavage (Sulston *et al.* 1983; Figure 9). Non-Unc-36 animals therefore necessarily carry *unc-36(+)* and *mnEx54* in at least some descendants of both ABpl and ABpr.

We exposed the progeny of *unc-36 ncl-1; osm-6; mnEx54* hermaphrodites to the fluorescent dye DiO, picked non-Unc-36 animals, mounted them on agar pads on microscope slides and screened for animals in which at least one amphid neuron, generally ASK, ADL or ASI, was Ncl. When a genetic mosaic was found, amphid neurons were scored with respect to both DiO filling and the Ncl phenotype. For several animals, we scored the Ncl phenotype of many additional cells to pinpoint positions in the lineage at which the extrachromosomal array was lost; one such mosaic animal is described by Figure 9.

All of the neurons and support cells—sheaths and sockets—of the amphid and phasmid sensilla are descendants of AB. In wild-type animals, six neurons of each amphid fill with DiO, but only four fill strongly. ASI fills very weakly and AWB fills somewhat weakly (Starich *et al.* 1995). We therefore scored the dye-filling properties of the four that fill strongly—ADL, ASH, ASJ and ASK—in mosaic animals. The results confirmed the prediction of cell autonomy for each of these four neurons. We scored a total of 80 neurons in 22 mosaic amphids with respect to both Ncl and Dyf phenotypes (in some cases the only Ncl neuron in a mosaic amphid was ASI, which was not scored with respect to dye filling, and in other cases, not all neurons were identified and scored): 21 neurons were Ncl and dye-filling negative, 58 were non-Ncl and filled with dye normally, and one exceptional neuron was Ncl and filled with dye weakly. The exceptional Ncl neuron exhibiting weak dye filling may have picked up its dye from dye-filled neighbors, although we saw other examples in which the same neuron, ADL, was surrounded by dye-filled neighbors and did not fill even weakly. The four neurons assayed for dye filling are not closely related by lineage (Figure 9); as a consequence, various classes of mosaic amphids were found, supporting our conclusion of cell autonomy. The different classes of mosaic also led us to conclude that the genotypes of the amphid sheath and socket cells had no effect on dye filling; thus, we found examples (and no counterexamples) in which a mutant sheath cell did not block dye filling of a wild-type neuron in the same sensillum, and we found examples (one of which is given in Figure 9) in which a wild-type sheath did not promote the dye filling of a mutant neuron.

DISCUSSION

The evidence that we have correctly identified *osm-6* molecularly is based, first, on the transformation rescue, by defined genomic fragments, of the *osm-6* dye-filling defective phenotype and, second, on the molecular characterization of the five known *osm-6* mutations. The region of genomic DNA necessary for rescue was delimited to a 2.9-kb segment that encodes the cDNA we characterized as representing the *osm-6* message. One end of the 2.9-kb segment was delimited by a rescuing genomic fragment that extended only 190 nucleotides upstream of the 5′ end of the cDNA. The other end was delimited by a rescuing *osm-6::gfp* construct that included all but the last 13 codons, including the natural termination codon, of the *osm-6* cDNA. As expected, the insertion of a frameshift mutation near the beginning of the open reading frame defined by the cDNA abolished the ability of a genomic fragment to rescue. Finally, each of the five *osm-6* mutant alleles was associated with an alteration that affected the coding capacity of the *osm-6* message. Two were transposon insertions within coding sequence, two affected consensus splice sites between coding exons, and one was a nonsense mutation of the amber class, which was suppressed by an amber suppressor. We conclude that we have identified *osm-6*.

We suggest that all five *osm-6* mutations are null or nearly null. All five mutations are recessive to *osm-6(+)* and abolish dye filling of amphid and phasmid neurons: *osm-6* opposite a deficiency has the same Dyf phenotype. The amber suppressor *sup-5*, when homozygous at 20°, restores approximately 10% of the wild-type level of expression to a suppressed locus (Waterston and Brenner 1978; Waterston 1981). When *osm-6(sa119)* was suppressed by *sup-5* at 20°, animals exhibited considerable dye filling, albeit not completely wild-type. (We also saw some dye filling in animals that

carried a single copy of the suppressor.) This indicates that *osm-6* mutations that reduced but did not abolish *osm-6* expression could permit some level of dye filling. The *osm-6* mutant phenotypes appear to be limited to chemosensory and mechanosensory defects; all mutants are fully viable and fertile and move with wild-type coordination. Our *osm-6::gfp* expression studies, which suggest that OSM-6 is produced only in ciliated neurons, are also consistent with the idea that *osm-6* function does not extend to cells other than the ciliated class of sensory neurons. Of course, we cannot exclude the possibility that *osm-6::gfp* is expressed at low but undetectable levels in nonciliated cells or that our construct is not accurately reflecting the wild-type pattern of *osm-6* expression; we also cannot exclude the possibility that *osm-6* provides a subtle or redundant function in nonciliated cells.

The best candidate for a null mutation on the basis of molecular evidence is *sa119*, a nonsense mutation at codon 377, which would omit 96 amino acid residues from the C-terminal end of the protein. Although omission of the last 12 amino acids did not block *osm-6* function in the *osm-6::gfp* construct, it seems likely that omission of the larger C-terminal segment would, particularly since most of it is similar to the mammalian NGD5 protein.

Tc1 insertion mutations within coding sequence are not invariably null. Splicing of the transcript from the Tc1-bearing gene can remove most or all of the Tc1 sequence to give messages that contain small insertions, deletions or substitutions, and some of these mature transcripts may contain in-frame mRNA that encodes protein with small deletions, insertions or substitutions of amino acid residues (Rushforth and Anderson 1996). If the function of the protein is tolerant of such alterations, then some residual function may be retained. We suggest that the two Tc1 insertions in *osm-6* are in regions (*m511* between codons 273 and 274 and *m533* between codons 180 and 181) that are intolerant of such changes.

Splice site mutations can also retain some residual function. Although the dinucleotide AG is found at the 3′ end of essentially all eukaryotic introns, Aroian *et al.* (1993) showed that when such AGs were mutated to AA in two *C. elegans* genes, each gene retained residual function by virtue of some correct splicing of the mutant intron, although a variety of incorrect splices were also made as a consequence of the mutations. Zhang and Blumenthal (1996) have observed some splicing to AA at the 3′ end of a synthetic intron. These workers also found that the efficiency of splicing to the AA was reduced when UUUC immediately 5′ of the AA dinucleotide was changed to UUCC; the latter sequence immediately precedes the AG to AA change at the 3′ end of the first intron in *p811*. Because it is not yet possible to predict with any confidence an expected pattern of splicing for the *p811* mutant, we cannot say from the molecular evidence that *osm-6(p811)* is null. Similarly, we cannot be sure from the molecular evidence that the 5′ splice site mutation, *m201*, is null. Although the 5′ end of the seventh intron of the *osm-6* transcript is changed from the virtually invariant GU to AU, Rushforth and Anderson (1996) have detected the use of an AU 5′ splice donor in the production of aberrant splice products by *unc-54* Tc1 insertion mutants.

Our mosaic analysis indicates that the effect of *osm-6* on the ability of amphid neurons to fill with dye is cell autonomous. We therefore suggest that the ultrastructural defects in *osm-6* sensory axonemes detected by electron microscopy (Perkins *et al.* 1986) are also cell autonomous. The *osm-6::gfp* expression results, which indicate that OSM-6 is a cytoplasmic protein present near sensory axonemes, clearly support this view. Perkins *et al.* (1986) observed an increased number of unfused matrix-filled vesicles in the cytoplasm of the amphid sheath cells in the *osm-6* mutant (as well as in other mutants with shortened cilia) compared to wild-type animals. The amphid sheath cell is a nonneuronal support cell that makes a cylindrical channel that surrounds a bundle of neuronal processes. Ciliated dendrites project into one end of the channel; the other end is extended by connection of the sheath to a nonneuronal socket cell and terminates at a pore to the outside. The wild-type sheath cell contains vesicle-bound material that is thought to be exported to the extracellular channel matrix (Perkins *et al.* 1986). We suggest that the presence of excess vesicles in *osm-6* sheath cells is a secondary consequence of the axonemal defect in the neighboring neurons and is not the cause of the ciliary defects; thus, a mutant sheath cell did not block normal dye filing by an *osm-6(+)* neuron in the same sensillum.

The presence of OSM-6::GFP near sensory cilia and its perturbed localization in these regions in various mutants with aberrant sensory cilia support the proposal of Perkins *et al.* (1986) that OSM-6 plays a role in promoting the growth of axonemes. In the absence of functional OSM-6 protein, the base and intermediate zones of the cilia appear to be normal, but the distal parts of the axonemes are foreshortened, and ectopic membrane-attached microtubules assemble at sites proximal to the cilia. It has been suggested that the ectopic microtubules are misassembled components of the foreshortened axoneme (Perkins *et al.* 1986). All cilia in the head of an *osm-6* mutant were found by electron microscopy to be defective (Perkins *et al.* 1986). In hermaphrodites carrying our *osm-6::gfp* construct, we detected expression of GFP by 56 ciliated neurons. The only ciliated neurons that did not show expression were two pairs in the head called BAG and FLP. It is possible that these neurons also require *osm-6* function and that either the level of expression was below our limit of detection or the *osm-6L::gfp* construct we used lacked a regulatory feature required for expression in

these cells. Additional cells exhibited GFP expression in males, including the ciliated CEM neurons in the head and several unidentified cells in the tail, some of which, at least, have endings in the male spicules and sensory rays. The pattern of OSM-6::GFP localization suggests that OSM-6 is itself a component of the sensory cilia. Consistent with this suggestion was our finding of reduced OSM-6::GFP localization in the dendritic endings of animals carrying mutations in *che-2*, *che-13*, *osm-1* and *osm-5*. All four of these mutants have foreshortened cilia, lacking middle and distal segments (Perkins *et al.* 1986). Also consistent with the idea that OSM-6 is a ciliary component was our observation that OSM-6::GFP accumulation was enhanced near the bundled endings of *che-3* amphid and phasmid neurons; the amphid and phasmid neurons in *che-3* mutants have been shown to have shortened but enlarged-diameter endings filled with electron-dense material (Lewis and Hodgkin 1977; Albert *et al.* 1981), which we suggest includes OSM-6 and other ciliary components.

Bargmann and Horvitz (1991b) showed that when ciliated amphid neurons ADF, ASG and ASI were killed early in the L1 stage, wild-type animals formed dauer larvae constitutively, *i.e.*, despite the presence of food. This finding indicates that these sensory neurons normally signal to present dauer formation in the presence of food. All cilium-defective mutants except *daf-19* retain this inhibitory function, since they do not form dauers under normal growth conditions. Indeed, when the sensory neurons were killed in the cilium-defective mutants *che-2* and *daf-10*, which are normally defective in dauer formation, they formed dauers constitutively (Bargmann and Horvitz 1991b). The exceptional cilium-defective *daf-19* mutant lacks cilia (Perkins *et al.* 1986), whereas the other mutants have malformed cilia, and rather than being defective in dauer formation, *daf-19* animals form dauers constitutively. Although it is possible that defects in cells other than the sensory neurons are responsible for the dauer constitutive phenotype of *daf-19* animals, it seems simpler to suppose that the sensory neurons are responsible. Possibly it is the complete absence of cilia in *daf-19* animals that leads to constitutive dauer formation. According to this view, the shortened cilia in *osm-6* mutants impair the ability to form dauer larvae under conditions of starvation and limited food, but retain enough ciliary function to repress inappropriate dauer formation. Another possibility is that *daf-19(+)* is required to specify at least two distinct sensory cell functions: the formation of cilia and the repression of inappropriate dauer formation. In any case, it is interesting that the accumulation of OSM-6-GFP is drastically curtailed in *daf-19* animals.

A corollary of our suggestion that *osm-6* serves the single role of promoting distal outgrowth of all sensory axonemes is the suggestion that all of the behavioral problems exhibited by *osm-6* animals—defective chemotaxis to various water soluble compounds and volatile odorants, defective dauer larvae formation, defective responses to touch in the head and poor male mating (Hodgkin 1983)—are caused, directly or indirectly, by defective sensory cilia. Different sets of sensory neurons are implicated in different behaviors, as noted in the introduction, but we suggest that all of these behaviors require intact cilia. Not all mechanosensation in *C. elegans* requires intact cilia; mechanosensory receptors in the body and tail of the animal are not ciliated (Chalfie and Sulston 1981), and *osm-6* animals do respond to touch along the body and in the tail.

We searched the OSM-6 amino acid sequence using the Motifs and ProfileScan programs of the Genetics Computer Group and did not identify any protein motifs or domains. We also applied the PHD program (Rost 1996) for predicting secondary structure; the most striking prediction was that the OSM-6 segment from residues 332 to 370 is devoid of both α-helix and β-strand. This segment includes most of the proline-rich region and overlaps almost exactly the longest region of high similarity (>75% identical) between OSM-6 and the NGD5 protein (Figure 5). We suggest that this segment may have domains that take on a threefold left-handed helical structure referred to as the left-handed poly-l-proline II (PPII) helix. Adzhubei and Sternberg (1993) have shown that PPII helices are common in globular proteins. Although not obligatory components of PPII helices, proline residues strongly favor their formation (Adzhubei and Sternberg 1993). Among the least favored amino acid residues in PPII helices are tryptophan, isoleucine, glycine, tyrosine, histidine and cysteine, all of which are absent from the 39-residue segment from residues 332 to 370. PPII helices tend to be exposed to solvent and are therefore thought to be ideal for interactions with other proteins (Adzhubei and Sternberg 1993; Cohen *et al.* 1995). Peptide regions that bind to SH3 domains have PPII helical structure (Feng *et al.* 1994; Lim *et al.* 1994; Lee *et al.* 1996). All SH3 binding sites that have been examined have a PxxP motif (Cohen *et al.* 1995), which is present twice in this region of OSM-6 and once in the corresponding region of the NGD5 protein. Residues surrounding the PxxP motif are thought to confer specificity of binding of the ligand to particular SH3 domains. The PxxP motif present in the NGD5 protein is embedded in a sequence that is very similar to the proposed consensus of one class of SH3 binding sequence, RxLPP(L/R)P (Feng *et al.* 1994). The SH3 domain, which contains approximately 60 amino acids, is found in a wide variety of proteins, including signal transduction proteins and cytoskeleton proteins such as spectrin (Cohen *et al.* 1995). Possibly OSM-6 binds to an SH3-containing cytoskeletal protein.

The original *NGD5* cDNA (Wick *et al.* 1995) was identified in a library constructed from a hybrid cell line, NG108-15, made from mouse neuroblastoma and

rat glioma cell lines. Northern blot analysis indicated that *NGD5* transcripts are present in both parental cell lines as well as rat brain. Neither NG108-15 cells (Daniels and Hamprecht 1974) nor rat PC12 cells (Greene and Tischler 1976), from which an *NGD5*-like cDNA was derived (Lee *et al.* 1995), appear to be ciliated. After the NG108-15 cells were exposed to an opioid agonist for 48 hr, the level of *NGD5* transcript was reduced to about 60% the pretreatment level. NG108-15 cells express high levels of opioid receptors, which mediate, in at least some cases through the action of GTP-binding regulatory proteins, a variety of physiological effects (Reisine and Bell 1993). Many ESTs—one derived from rat, two from mouse and more than a dozen from a variety of human tissues—have been identified that are very similar to *NGD5*. NGD5 protein has not been identified, and its function is unknown. We suggest from our work on OSM-6 that it may interact with the cytoskeleton, perhaps through the proline-rich region that is highly similar to OSM-6.

We thank T. Starich for much good advice; C. Kari for able technical help; C. Link, R. Barstead, R. Waterston and S. Kim for genomic and cDNA libraries; A. Fire for the *gfp* vector and the *rp21* clone; L. Lobel for an *unc-36(+)*-bearing plasmid; M. Wick for the clone *NGD5*; and A. Coulson for putting *osm-6* on the physical map. This work was supported by National Institutes of Health (NIH) research grants HD22163 (J.E.S.) and GM22387 (R.K.H.). J.C. was a recipient of a fellowship from the Catalonian Commissionat per a Universitats i Recerca. Some nematode strains were supplied by the *Caenorhabditis* Genetics Center, which is supported by a contract between the NIH National Center for Research Resources and the University of Minnesota.

LITERATURE CITED

Adzhubei, A. A., and M. J. E. Sternberg, 1993 Left-handed polyproline II helices commonly occur in globular proteins. J. Mol. Biol. **229:** 472–493.

Albert, P. S., S. J. Brown and D. L. Riddle, 1981 Sensory control of dauer larva formation in *Caenorhabditis elegans*. J. Comp. Neurol. **198:** 435–451.

Albertson, D. G., and J. N. Thomson, 1976 The pharynx of *Caenorhabditis elegans*. Phil. Trans. R. Soc. Lond. B. **275:** 299–325.

Altschul, S. F., W. Gish, W. Miller, E. W. Myers and D. J. Lipman, 1990 Basic local alignment search tool. J. Mol. Biol. **215:** 403–410.

Anderson, P., 1995 Mutagenesis, pp. 31–58 in *Caenorhabditis elegans: Modern Biological Analysis of an Organism*, edited by H. F. Epstein and D. C. Shakes. Academic Press, San Diego.

Aroian, R. V., A. D. Levy, M. Koga, Y. Ohshima, J. M. Kramer *et al.*, 1993 Splicing in *Caenorhabditis elegans* does not require an AG at the 3′ splice acceptor site. Mol. Cell. Biol. **13:** 626–637.

Bargmann, C. I., and H. R. Horvitz, 1991a Chemosensory neurons with overlapping functions direct chemotaxis to multiple chemicals in *C. elegans*. Neuron **7:** 729–742.

Bargmann, C. I., and H. R. Horvitz, 1991b Control of larval development of chemosensory neurons in *Caenorhabditis elegans*. Science **251:** 1243–1246.

Bargmann, C. I., and I. Mori, 1997 Chemotaxis and thermotaxis, pp. 717–737 in *C. elegans II*, edited by D. L. Riddle, T. Blumenthal, B. J. Meyer and J. R. Priess. Cold Spring Harbor Laboratory, Cold Spring Harbor, NY.

Bargmann, C. I., J. H. Thomas and H. R. Horvitz, 1990 Chemosensory cell function in the behavior and development of *Caenorhabditis elegans*. Cold Spring Harb. Symp. Quant. Biol. **55:** 529–538.

Bargmann, E. I., E. Hartwieg and H. R. Horvitz, 1993 Odorant-selective genes and neurons mediate olfaction in *C. elegans*. Cell **74:** 515–527.

Blumenthal, T., and K. Steward, 1997 RNA processing and gene structure, pp. 117–145 in *C. elegans II*, edited by D. L. Riddle, T. Blumenthal, B. J. Meyer and J. R. Priess. Cold Spring Harbor Laboratory, Cold Spring Harbor, NY.

Brenner, S., 1974 The genetics of *Caenorhabditis elegans*. Genetics **77:** 71–94.

Cassada, R. C., and R. L. Russell, 1975 The dauer larva, a post-embryonic developmental variant of the nematode *Caenorhabditis elegans*. Dev. Biol. **46:** 326–342.

Chalfie, M., and J. Sulston, 1981 Developmental genetics of the mechanosensory neurons of *Caenorhabditis elegans*. Dev. Biol. **82:** 358–370.

Chalfie, M., Y. Tu, G. Euskirchen, W. W. Ward and D. C. Prasher, 1994 Green fluorescent protein as a marker for gene expression. Science **263:** 802–805.

Chow, K. L., D. H. Hall and S. W. Emmons, 1995 The *mab-21* gene of *Caenorhabditis elegans* encodes a novel protein required for choice of alternate cell fates. Development **121:** 3615–3626.

Cohen, G. B., R. Ren and D. Baltimore, 1995 Modular binding domains in signal transduction proteins. Cell **80:** 237–248.

Coulson, A., C. Huynh, Y. Kozono and R. Shownkeen, 1995 The physical map of the *Caenorhabditis elegans* genome, pp. 534–550 in *Caenorhabditis elegans: Modern Biological Analysis of an Organism*, edited by H. F. Epstein and D. C. Shakes. Academic Press, San Diego.

Culotti, J. G., and R. L. Russell, 1978 Osmotic avoidance defective mutants of the nematode *Caenorhabditis elegans*. Genetics **90:** 243–256.

Daniels, M. P., and B. Hamprecht, 1974 The ultrastructure of neuroblastoma glioma somatic cell hybrids. J. Cell Biol. **63:** 691–699.

Feng, S., J. K. Chen, J. Yu, J. A. Simon and S. L. Schreiber, 1994 Two binding orientations for peptides to the Src SH3 domain: development of a general model for SH3–ligand interactions. Science **266:** 1241–1247.

Greene, L. A., and A. S. Tischler, 1976 Establishment of a noradrenergic clonal line of rat adrenal pheochromocytoma cells which respond to nerve growth factor. Proc. Natl. Acad. Sci. USA **73:** 2424–2428.

Hall, D. H., and R. L. Russell, 1991 The posterior nervous system of the nematode *Caenorhabditis elegans*: serial reconstruction of identified neurons and complete pattern of synaptic interactions. J. Neurosci. **11:** 1–22.

Hedgecock, E. M., and R. K. Herman, 1995 The *ncl-1* gene and genetic mosaics of *Caenorhabditis elegans*. Genetics **141:** 989–1006.

Hedgecock, E. M., J. G. Culotti, J. N. Thomson and L. A. Perkins, 1985 Axonal guidance mutants of *Caenorhabditis elegans* identified by filling sensory neurons with fluorescein dyes. Dev. Biol. **111:** 158–170.

Henikoff, S., 1987 Unidirectional digestion with exonuclease III in DNA sequence analysis. Methods Enzymol. **155:** 156–157.

Hodgkin, J., 1983 Male phenotypes and mating efficiency in *Caenorhabditis elegans*. Genetics **103:** 43–64.

Hodgkin, J., M. Edgley, D. L. Riddle and D. G. Albertson, 1988 Genetics, pp. 491–584 in *The Nematode Caenorhabditis elegans*, edited by W. B. Wood. Cold Spring Harbor Laboratory, Cold Spring Harbor, NY.

Horvitz, H. R., S. Brenner, J. Hodgkin and R. K. Herman, 1979 A uniform genetic nomenclature for the nematode *Caenorhabditis elegans*. Mol. Gen. Genet. **175:** 129–133.

Johnson, K. A., 1995 Keeping the beat: form meets function in the *Chlamydomonas* flagellum. Bioessays **17:** 847–854.

Kaplan, J. M., and H. R. Horvitz, 1993 A dual mechanosensory and chemosensory neuron in *Caenorhabditis elegans*. Proc. Natl. Acad. Sci. USA **90:** 2227–2231.

Kenyon, C. J., 1986 A gene involved in the development of the posterior body region of *Caenorhabditis elegans*. Cell **46:** 477–487.

Krause, M., 1995 Transcription and translation, pp. 483–512 in *Caenorhabditis elegans: Modern Biological Analysis of an Organism*, edited by H. F. Epstein and D. C. Shakes. Academic Press, San Diego.

Kyte, J., and R. F. Doolittle, 1982 A simple method for displaying the hydropathic character of a protein. J. Mol. Biol. **157:** 105–132.

Lee, C.-H., K. Saksela, U. A. Mirza, B. T. Chait and J. Kuriyan, 1996 Crystal structure of the conserved core of HIV-1 Nef complexed with a Src family SH3 domain. Cell **85:** 931–942.

Lee, N. H., K. G. Weinstock, E. F. Kirkness, J. A. Earle-Hughes, R. A. Fuldner *et al.*, 1995 Comparative expressed-sequence-tag analysis of differential gene expression profiles in PC-12 cells before and after nerve growth factor treatment. Proc. Natl. Acad. Sci. USA **92:** 8303–8307.

Lewis, J. A., and J. A. Hodgkin, 1997 Specific neuroanatomical changes in chemosensory mutants of the nematode *Caenorhabditis elegans*. J. Comp. Neurol. **172:** 489–510.

Li, W., R. K. Herman and J. E. Shaw, 1992 Analysis of the *Caenorhabditis elegans* axonal guidance and outgrowth gene *unc-33*. Genetics **132:** 675–689.

Lim, W. A., F. M. Richards and R. O. Fox, 1994 Structural determinants of peptide-binding orientation and of sequence specificity in SH3 domains. Science **372:** 375–379.

Mello, C. C., and A. Fire, 1995 DNA transformation, pp. 451–482 in *Caenorhabditis elegans: Modern Biological Analysis of an Organism*, edited by H. F. Epstein and D. C. Shakes. Academic Press, San Diego.

Mello, C. C., J. M. Kramer, D. Stinchcomb and V. Ambros, 1991 Efficient gene transfer in *C. elegans*: extrachromosomal maintainance and integration of transforming sequences. EMBO J. **10:** 3959–3970.

Miller, L. M., D. A. Waring and S. K. Kim, 1996 Mosaic analysis using a *ncl-1(+)* extrachromosomal array reveals that *lin-31* acts in the Pn.p cells during *Caenorhabditis elegans* vulval development. Genetics **143:** 1181–1191.

Mori, I., D. G. Moerman and R. H. Waterston, 1988 Analysis of a mutator activity necessary for germline transposition and excision of Tc1 transposable elements in *Caenorhabditis elegans*. Genetics **120:** 397–407.

Nelson, G. A., and S. Ward, 1980 Vesicle fusion, pseudopod extension and amoeboid motility are induced in nematode spermatids by the ionophore monensin. Cell **19:** 457–464.

Perkins, L. A., E. M. Hedgecock, J. N. Thomson and J. G. Culotti, 1986 Mutant sensory cilia in the nematode *Caenorhabditis elegans*. Dev. Biol. **117:** 456–487.

Reisine, T., and G. I. Bell, 1993 Molecular biology of opioid receptors. Trends Neurosci. **16:** 504–510.

Riddle, D. L., and P. S. Albert, 1997 Genetic and environmental regulation of dauer larva development, pp. 739–768 in *C. elegans II*, edited by D. L. Riddle, T. Blumenthal, B. J. Myer and J. R. Priess. Cold Spring Harbor Laboratory, Cold Spring Harbor, NY.

Rosenzweig, B., L. W. Liao and D. Hirsh, 1983 Target sequences of the *Caenorhabditis elegans* transposable element Tc1. Nucleic Acids Res. **11:** 7137–7140.

Rost, B., 1996 PHD: predicting one-dimensional protein structure by profile-based neural networks. Methods Enzymol. **266:** 525–539.

Rushforth, A. M., and P. Anderson, 1996 Splicing removes the *Caenorhabditis elegans* transposon Tc1 from most mutant pre-mRNAs. Mol. Cell. Biol. **16:** 422–429.

Sambrook, J., E. F. Fritsch and T. Maniatis, 1989 *Molecular Cloning: A Laboratory Manual*, Ed. 2. Cold Spring Harbor Laboratory, Cold Spring Harbor, NY.

Sanger, F., S. Nicklen and A. R. Coulson, 1977 DNA sequencing with chain-terminating inhibitors. Proc. Natl. Acad. Sci. USA **74:** 5463–5467.

Schackwitz, W. S., T. Inoue and J. H. Thomas, 1996 Chemosensory neurons function in parallel to mediate a pheromone response in *C. elegans*. Neuron **17:** 719–728.

Starich, T. A., R. K. Herman and J. E. Shaw, 1993 Molecular and genetic analysis of *unc-7*, a *Caenorhabditis elegans* gene required for coordinated locomotion. Genetics **133:** 527–541.

Starich, T. A., R. K. Herman, C. K. Kari, W.-H. Yeh, W. S. Schackwitz *et al.*, 1995 Mutations affecting the chemosensory neurons of *Caenorhabditis elegans*. Genetics **139:** 171–188.

Sulston, J., and J. Hodgkin, 1988 Methods, pp. 587–606 in *The Nematode Caenorhabditis elegans*, edited by W. B. Wood. Cold Spring Harbor Laboratory, Cold Spring Harbor, NY.

Sulston, J. E., and H. R. Horvitz, 1977 Postembryonic cell lineages of the nematode *Caenorhabditis elegans*. Dev. Biol. **56:** 110–156.

Sulston, J., and J. White, 1988 Parts list, pp. 415–431 in *The Nematode Caenorhabditis elegans*, edited by W. B. Wood. Cold Spring Harbor Laboratory, Cold Spring Harbor, NY.

Sulston, J. E., D. G. Albertson and J. N. Thomson, 1980 The *Caenorhabditis elelgans* male: postembryonic development of nongonadal structures. Dev. Biol. **78:** 542–576.

Sulston, J. E., E. Schierenberg, J. G. White and J. N. Thomson, 1983 The embryonic cell lineage of the nematode *Caenorhabditis elegans*. Dev. Biol. **100:** 64–119.

Tabish, M., Z. K. Siddiqui, K. Nishikawa and S. S. Siddiqui, 1995 Exclusive expression of *C. elegans osm-3* kinesin gene in chemosensory neurons open to the external environment. J. Mol. Biol. **247:** 377–389.

Thomas, J. H. 1993 Chemosensory regulation of development in *C. elegans*. BioEssays **15:** 791–797.

Van Luenen, H. G. A. M., and R. H. A. Plasterk, 1994 Target site choice of the related transposable elements Tc1 and Tc3 of *Caenorhabditis elegans*. Nucleic Acids Res. **22:** 262–269.

Ward, S., J. N. Thomson, J. G. White and S. Brenner, 1975 Electron microscopical reconstruction of the anterior sensory anatomy of the nematode *Caenorhabditis elegans*. J. Comp. Neurol. **160:** 313–338.

Ware, R. W., D. Clark, K. Crossland and R. L. Russell, 1975 The nerve ring of the nematode *Caenorhabditis elegans*: sensory input and motor output. J. Comp. Neurol. **162:** 71–110.

Waterston, R. H., 1981 A second informational suppressor, *sup-7 X*, in *Caenorhabditis elegans*. Genetics **97:** 307–325.

Waterston, R. H., and S. Brenner, 1978 A suppressor mutation in the nematode acting on specific alleles of many genes. Nature **275:** 715–719.

White, J. G., E. Southgate, J. N. Thomson and S. Brenner, 1986 The structure of the nervous system of *Caenorhabditis elegans*. Phil. Trans. R. Soc. Lond. B. **314:** 1–340.

Wick, M. J., D. K. Ann and H. H. Loh, 1995 Molecular cloning of a novel protein regulated by opioid treatment of NG108-15 cells. Mol. Brain Res. **32:** 171–175.

Wilson, R., R. Ainscough, K. Anderson, C. Baynes, M. Berks *et al.*, 1994 2.2 Mb of contiguous nucleotide sequence from chromosome III of *C. elegans*. Nature **368:** 32–38.

Wolf, N., D. Hirsh and J. R. McIntosh, 1978 Spermatogenesis in males of the free-living nematode, *Caenorhabditis elegans*. J. Ultrastruct. Res. **63:** 155–169.

Zhang, H., and T. Blumenthal, 1996 Functional analysis of an intron 3′ splice site in *Caenorhabditis elegans*. RNA **2:** 380–388.

Communicating editor: I. Greenwald